Available online at www.sciencedirect.com

ScienceDirect

Transportation Research Procedia 7 (2015) 320 – 340

Transportation Research Procedia

www.elsevier.com/locate/procedia

21st International Symposium on Transportation and Traffic Theory

Optimal transit service atop ring-radial and grid street networks: a continuum approximation design method and comparisons

Haoyu Chen [a,*], Weihua Gu [b], Michael Cassidy [a], Carlos Daganzo [a]

[a] *University of California, Berkeley, 416 McLaughlin Hall, Berkeley, CA, 94720, USA*
[b] *The Hong Kong Polytechnic University, CF612, Hunghom, Kowloon, HK*

Abstract

Two continuum approximation (CA) optimization models are formulated to design city-wide transit systems at minimum cost. Transit routes are assumed to lie atop a city's street network. Model 1 assumes that the city streets are laid out in ring-radial fashion. Model 2 assumes that the city streets form a grid. Both models can furnish hybrid designs, which exhibit intersecting routes in a city's central (downtown) district and only radial branching routes in the periphery. Model 1 allows the service frequency and the route spacing at a location to vary arbitrarily with the location's distance from the center. Model 2 also allows such variation but in the periphery only.

The paper shows how to solve these CA optimization problems numerically, and how the numerical results can be used to design actual systems. A wide range of scenarios is analyzed in this way. It is found among other things that in all cases and for both models: (i) the optimal headways and spacings in the periphery increase with the distance from the center; and (ii) at the boundary between the central district and the periphery both, the optimal service frequency and line spacing for radial lines decrease abruptly in the outbound direction. On the other hand Model 1 is distinguished from Model 2 in that the former produces in all cases: (i) a much smaller central district, and (ii) a high frequency circular line on the outer edge of the central district.

Parametric tests with all the scenarios further show that Model 1 is consistently more favorable to transit than Model 2. Cost differences between the two designs are typically between 9% and 13%, but can top 21.5%. This is attributed to the manner in which ring-radial networks naturally concentrate passenger's shortest paths, and to the economies of demand concentration that transit exhibits. Thus, it appears that ring-radial street networks are better for transit than grids.

In order to illustrate the robustness of the CA design procedure to irregularities in real street networks, the results for all the test problems were then used to design and evaluate transit systems on networks of the "wrong" type – grid networks were outfilled with transit systems designed with Model 1 and ring-radial networks designed with Model 2. Cost increased on average by a little 2.7%. The magnitude of these deviations suggests that the proposed CA procedures can be used to design transit systems over real street networks when they are not too different from the ideal and that the resulting costs should usually be very close to those predicted.

Selection and peer-review under responsibility of Kobe University

Keywords: transit network; continuum approximation method

* Haoyu Chen. Tel.: +1-510-642-7702 ; fax: +1-510-643-8919.
E-mail address: haoyuchen@berkeley.edu

Selection and peer-review under responsibility of Kobe University
doi:10.1016/j.trpro.2015.06.017

1. Introduction

Idealized models have long been used to determine how transit networks should be organized. Holroyd (1967) appears to be the first work to have examined a city-wide system. It explored how a bus grid should be organized in terms of its vehicle headways and station spacings so as to provide optimum service for a given cost. Other works subsequently analyzed other network structures, including those that are purely radial and purely ring-and-radial in form (Byrne, 1975; Black, 1979; Vaughan, 1986).

More recently, Daganzo (2010) examined a hybrid structure that serves a city by means of a square grid of transit routes within a central (e.g. downtown) district, in combination with radial routes that branch throughout the periphery. This hybrid structure generalizes those previously studied. The structure is fully described by just three parameters: the station spacing, which was assumed to be even over the entire city; the vehicle headway in the central district; and the physical size of that district relative to the size of the entire city. The model unveiled how distinct transit modes (bus, BRT and rail) can serve distinct city forms. The hybrid concept was more recently adapted to ring-radial transit networks in Badia, et al. (2014).

All but one of the models cited above (Vaughan, 1986) can be improved by allowing headways and line spacings to vary with location, so that they can be better adapted to a city's travel demand. A nice way of doing this is with continuum approximations (CAs) of the type first proposed in Newell (1971, 1973). In the context of transit, the CA method models station and route spacings as continuous functions of location. Similarly, headways are treated as a continuous function of location and time. Example applications include: Newell (1971), which modeled a single transit station with time-dependent demand; Wirasinghe and Ghoneim (1981), which modeled a corridor; Clarens and Hurdle (1975), which modeled a many-to-one system; and Vaughan (1986).

The above examples illustrate how the design problem can be greatly simplified by modeling a system's numerous decision variables with just a few decision functions. By virtue of these simplifications, the CA models take-on idealized qualities. Yet, their outputs can serve as guidelines for designing actual transit systems in real-world settings. The design objective is a system that fits a city's street layout and achieves costs close to those predicted by adhering to the guidelines as closely as possible. Some design examples with cost comparisons for many-to-one problems can be found in Clarens and Hurdle (1975) and Ouyang and Daganzo (2006).

Despite their favorable attributes, Vaughan (1986) appears to be the only previous attempt to use CA methods to design a many-to-many system with spatially varying headways and line spacings. That model minimizes passenger trip time subject to a fleet size constraint. It looks for an optimum ring-radial transit system atop a dense ring-radial street network, but the model does not allow for a hybrid structure and lacks realism by allowing for arbitrary headway functions, which require numerous transfers, and then ignoring passenger waiting times while transferring.[1]

Two CA models are developed in the present paper that correct this flaw and generalize both Vaughan (1986) and Daganzo (2010). Like Vaughan (1986), Model 1 assumes a circular city with a dense ring-radial street network. It generalizes this reference by allowing for a hybrid transit structure that features both ring and radial lines in the central district, and radial lines alone in the city's periphery. Like Daganzo (2010), Model 2 assumes a square city with a dense square grid of streets. Model 2 generalizes that reference by allowing headways and line spacings to vary within the periphery.

Section 2 below presents the two model formulations and the numerical procedures to optimize the designs. Sections 3 and 4 apply these procedures to a battery of problems in order to: (i) unveil generic properties of the optimum designs (Sec. 3); and (ii) evaluate their costs (Sec. 4).

2. Models

This section presents the models and the analysis methods. Subsections 2.1 and 2.2 introduce the basic assumptions: Sec 2.1 for supply and Sec. 2.2 for demand. Then, Sec. 2.3 formulates the problems and Sec. 2.4 discusses how to solve them.

[1] Non monotonic headway functions require that each radial line be served by multiple transit routes with distinct start and end points. As a result, many patrons must transfer between those routes when traveling radially. This phenomenon needs to be properly captured in a model that accounts for transfer times.

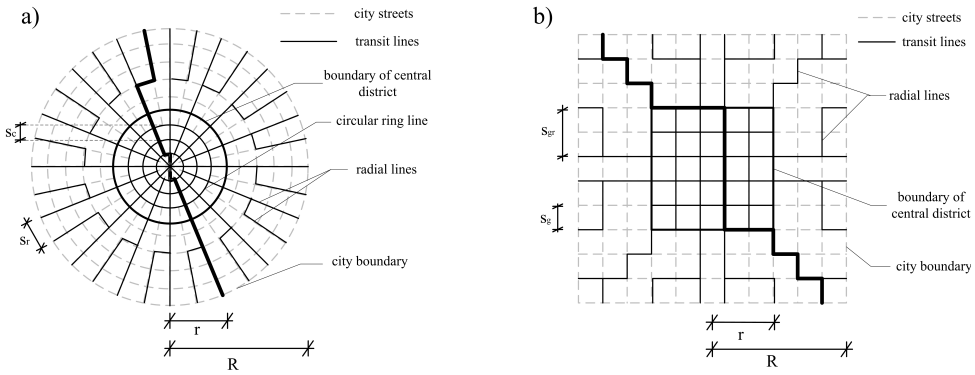

Fig. 1. (a) circular city and its ring-radial transit network; (b) square city and its grid transit network.

2.1. City Forms and the Supply of Transit

This subsection introduces notation and explains the assumptions regarding the structure of the transit systems. This is done first for Model 1 and then for Model 2.

It is assumed for Model 1 that the city is circular with radius R, and that its streets form a dense and rotationally-symmetric network; see Fig. 1a. It is also assumed that the city has a central district of radius r (to be determined) which enjoys double-coverage transit service; i.e. such that every point is near two transit lines – one circular and one radial. The headways on the circular ring lines and the spacings between these lines shall be denoted (H_c, s_c). Similarly, the headways and spacings pertaining to the radial routes shall be denoted (H_r, s_r).

The four headway and line spacing values at a location (H_c, s_c, H_r, s_r) are allowed to vary with the location's distance from the center, x, as in Vaughan (1986). Now, however, these functions are constrained to ensure that all patrons can travel in the radial direction without any transfers. Transfers are avoided by stipulating that all transit vehicles that travel along radial routes: (i) depart from a city's boundary; (ii) travel through the central district; and (iii) eventually arrive at the city boundary on the opposite side of town. This is illustrated by the route shown in bold in Fig. 1a. Since vehicles are dispatched at the city's boundary and conserved, the radial flow of buses across any circular ring, $\left(\frac{2\pi x}{s_r(x)}\right)\left(\frac{1}{H_r(x)}\right)$, must then be the same for all x;[2] i.e. $s_r(x)$ and $H_r(x)$ must satisfy the following conservation constraint:

$$\frac{2\pi R}{s_r(R)H_r(R)} = \frac{2\pi x}{s_r(x)H_r(x)}, \forall x \tag{1}$$

Lines with spacings that approximately conform to $s_r(x)$ are deployed by allowing outbound radial lines to bifurcate and inbound lines to merge; e.g., as in Fig. 1a.[3]

Consider now Model 2 and Fig. 1b. As in the figure, cities are assumed to be square with "radius" R (side $2R$) and to have a dense, square grid street system. As with Model 1, a central district of "radius" r (side $2r$) enjoys double coverage. In this case this coverage is achieved by lines forming a homogenous square grid with spacing s_g and sharing a common headway H_g. The radial routes in the periphery are prolongations of the central routes that extend all the way to the edge of the city; see the figure. Their headways and spacings are denoted (H_r, s_r). The latter are allowed to be arbitrary functions of the distance from the city center, where such distance is measured by the "radius" x of the square ring at each location. As with Model 1, (H_r, s_r) are related by the vehicle conservation constraint (1); and as in that model, line spacings that approximately conform to $s_r(x)$ are achieved by bifurcating routes.

[2] The factor $\frac{2\pi x}{s_r(x)}$ is the number of radial lines across the ring at x, and $\frac{1}{H_r(x)}$ is the bus flow on each radial line at x. Thus, $\frac{2\pi x}{s_r(x)H_r(x)}$ is the radial flow of buses across the ring at x.

[3] Route bifurcation/convergence is shown in the figure in abrupt, piecewise fashion, as might occur in real settings when transit lines are fit to underlying streets. Because we assume a continuum (as if a city's streets were infinitely dense), our numerical analyses will produce approximations in which bifurcations and convergences occur gradually over space; see Figs. 3 and 4.

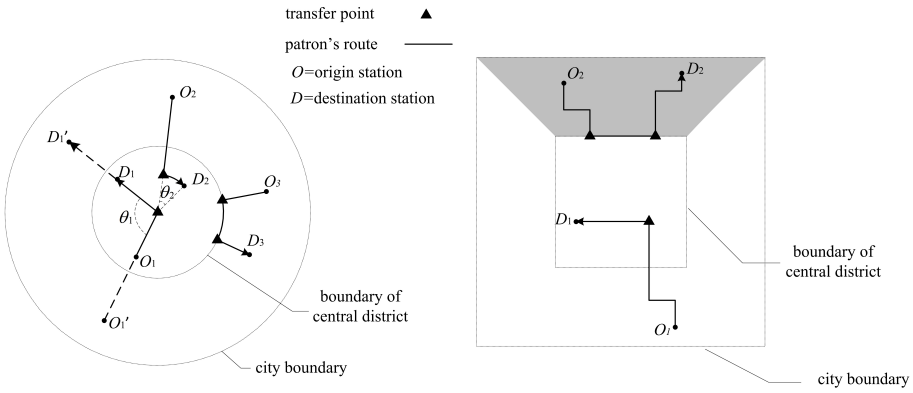

Fig. 2. (a) route choice for ring-radial network; (b) route choice for grid network.

2.2. Demand: Patron Choices of Routes and Transfers

It is assumed in this paper that the demand is temporally variable but spatially uniform; i.e., with origins and destinations uniformly and independently distributed in the interior of the city.[4] As explained in Daganzo (2010), temporal variations can be described for modeling purposes with only two parameters: the average daily demand and the rush-period rate. Furthermore, because the latter plays only a secondary role (it is just used to determine fleet size and the vehicles' passenger-carrying capacity) and to avoid the proliferation of parameters, this paper will fix the rush period demand at 250% of the average, just as in Daganzo (2010). Thus, the demand is fully characterized in the present paper by a single parameter: the trip generation rate per unit area, ρ (trips/hr-km^2).

Regarding travel behavior, it is assumed that a patron walks from her origin to the nearest transit station at speed, w (km/h), and ultimately departs the system via the station nearest her destination. It is further assumed that the patron chooses the transit route that offers the shortest trip distance, and breaks ties by first minimizing transfers and then choosing randomly among all the routes that remain. This is now fleshed out in more detail for each model.

Consider Model 1 and let θ be the angle (in radians) between the patron's origin and destination radii; e.g. see the trip labeled 1 in Fig. 2a. Consideration shows that if $\theta > 2$, a patron on a ring-radial network will travel by radial line to the city center and transfer there to another radial line to reach her destination. If instead $\theta < 2$, a patron will travel via both circular and radial lines, using the circle that is closest to the trip terminus that is itself closest to the city center. Proofs can be found in Holroyd (1967). This travel behavior is exemplified by trips 2 and 3 in the figure. Note in particular trip 3 in which a patron's origin and destination both lie in the periphery, such that two transfers are required. All other trip types require only one transfer.[5]

On hybrid grid networks, the routing pattern and transfers are as described in Daganzo (2010). Travelers use two intersecting routes if the trip can be achieved with only one transfer, in which case distance is minimized; or else using the three routes that minimize travel distance, and transferring twice in the process. As illustrated by Fig. 2b, the latter situation arises when a patron's origin and destination lie in the same quarter of the periphery. Consideration shows that it also arises if the origin and destination lie on opposite quarters of the periphery, and that all other origin-destination locations require only one transfer.

2.3. Model Formulations

We concern ourselves with the system's generalized cost in the city per unit time, denoted Z(\$/hour). This cost is the sum of the costs experienced by the transit agency, the public at large (externalities) and the system's users. These

[4] Though the proposed models can be extended to accommodate spatially inhomogeneous demands patterns with rotational symmetry, this is not done for the sake of simplicity.

[5] We conservatively ignore the small likelihood that a trip can be made without requiring a single transfer.

cost types are further subdivided into categories, i, that depend in a similar way on the decision variables. Thus, we write: $Z = \sum_i Z_i$, where the subscript i denotes a specific cost category.

For the transit agency three categories are considered: infrastructure, rolling stock operation and rolling stock capital. These costs depend on specific features of the system configuration, i.e., our design. The infrastructure cost is assumed to depend linearly on the total length of the transit routes, L; the rolling stock operating cost to depend linearly on the vehicle kilometers traveled per unit time, V; and the rolling stock capital cost on the fleet size M. For convenience these variables will be used to label the categories, so for the agency $i = L, V$ or M.

It seems reasonable to assume that the system's externalities are linked to what the agency does for this reason can be approximately expressed as a linear combination of L, V and M. As such, the external costs can be grouped together with the agency costs without involving any extra system configuration features if appropriate coefficients are chosen in the cost function. In other words, it is assumed that the two costs together are: $\$_L L + \$_V V + \$_M M$.

For the patrons, we recognize four cost categories: the access cost of walking to and from the origin and destination stations; the cost of waiting to board at the origin station and at transfer stations; the in-vehicle cost of riding from origin station to destination station; and a transfer penalty. These costs can also be related to the system design through some key variables. As the access cost is assumed to be proportional to the total distance walked per hour A, the waiting cost to the total time waited per hour, W, the in-vehicle travel cost to the total in-vehicle time per hour, T, and the transfer penalty to the total number of transfers done per hour, e_T. So as in the case of the agency cost and the externalities, the total user cost can be expressed as a linear combination of these variables: $\$_A A + \$_W W + \$_T T + \$_{e_T} e_T$. It will be assumed in the numerical examples that $\$_A = \$_W = \$_T = \mu$, where μ is a value of time that would be reasonable for an application.[6]

In summary, if we use Y_i for the design variables (L, V, M, A, W, T, e_T) and $\$_i$ for the cost coefficients, the systems' total cost is: $Z = \sum_i Z_i = \sum_i \$_i Y_i$. In agreement with the CA modeling framework we further break-down each of the above categories into: a set of localized cost densities, $z_i(x) = \$_i y_i(x)$ (\$/time-distance), that are associated with the circular crowns defined by radii $(x, x + dx)$, and that can be summed across all crowns from $x = 0$ to $x = R$; and a set of global fixed costs, F_i (\$/time). Thus we write:

$$Y_i = F_i + \int_0^R y_i(x)dx$$

The generalized cost to be minimized is therefore:

$$Z = \sum_i Z_i = \sum_i \$_i \left[F_i + \int_0^R y_i(x)dx\right] = \$_i \left[\sum_i F_i\right] + \$_i \left[\int_0^R \sum_i y_i(x)dx\right]$$

Appendices A and B explain how the F_i and y_i depend on the parameters of the problem and on the decision variables. The problem parameters are: R (or the area of the city, S); the demand density for trips, ρ(patrons/h/km^2); the transit vehicle's passenger-carrying capacity, C_{pax} and cruise speed, v(km/h);[7] the fixed lost time spent at stations due to acceleration, deceleration and doors opening and closing, τ(h/station), and the added time for each patron's boarding time, τ'(h/patron). (Alighting times are not considered, since these tend to be small and because boarding and alighting movements often occur simultaneously through separate doors.) Recall that the decision variables are the spacings, headways and the central district radius. In what follows only the dependence on the decision variables is important so this dependence is now explicitly expressed.

It will be convenient to separate the decision variables into a set of global variables, G, and a set of location-dependent decision functions of $x, D(x)$. The local decision functions are $D(x) = \{s_r(x), H_r(x), s_c(x), H_c(x)\}$ for ring-radial Model 1, and $D(x) = \{s_r(x), H_r(x)\}$ for grid Model 2. These functions define the system in those parts of the city where spacings and headways are allowed to vary.

The global decision variables define the general characteristics of the system. These include the radius of the central district, r, and an auxiliary variable, Q, which shall denote the flow of radial-line buses across every ring. The global variables also include the service headway, H_B, of the outermost ring route, i.e. the route on the boundary between the central district and the periphery, which is allowed to be smaller than $H_c(r)$. The special treatment of

[6] It would be possible to value the different components of travel time differently but this is not done to avoid the proliferation of parameters.

[7] This speed accounts for disruptions from traffic signals and other interferences along a route, but not for the stops made to serve demand. It depends on the type of technology and infrastructure used.

this ring route is justified because this is the only route that serves as a circulator for trips starting and ending in the periphery and therefore carries extra traffic. We shall also define an auxiliary variable for this route, s_B , representing the spacing between the route's stops that reside at the intersections of the radial lines and the boundary route. We will require that $s_B = s_r(r)$, however. It will be convenient to jointly refer to the two parameters for the boundary route as $f_B = (s_B, H_B)$. Finally, two additional variables are required for Model 2 (because this model has fewer local decision functions): the uniform spacing in the central district, s_g , and the common headway, H_g. It will be convenient to refer to these variables as $f_G = (s_g, H_g)$ and to define $f_G = \emptyset$ for ring-radial Model 1. In summary, the global decision variables are:

$$G = \{Q, r, f_B, f_G\} \text{ where } f_B = (s_B, H_B) \text{ and } f_G = \emptyset \text{ for Model 1 or } f_G = (s_g, H_g) \text{ for Model 2.}$$

Appendices A and B show that for both Models the elements of the objective function depend on the decision variables as indicted in the problem formulation below:

$$\min_{D(x),\, G}\{Z = \textstyle\sum_i \$_i[F_i(r, f_B, f_G)] + \int_0^R \sum_i \$_i[y_i(D(x), r, x)]dx\} \tag{2}$$

The appendices also show that the decision variables are constrained by the following relations, where C, C_G and K are functions of the indicated variables:

$$s_B = s_r(r) \quad \text{(definitional)} \tag{3a}$$

$$H_B \le H_c(r) \quad \text{(definitional for ring-radial network) or } H_B \le H_g \quad \text{(definitional for grid network)} \tag{3b}$$

$$C(D(x), x, Q) = 0, \ \ \forall x \ge r \quad \text{(vehicle conservation constraint)}^8 \tag{3c}$$

$$C_G(f_G, Q) = 0, \quad \text{(vehicle conservation constraint in central district, Model 2)} \tag{3d}$$

$$C(D(x), x, Q) = 0, \ \ \forall x < r \quad \text{(vehicle conservation constraint in central district, Model 1)} \tag{3e}$$

$$K(D(x), x) \le 0, \forall x \quad \text{(vehicle's passenger-carrying capacity constraint)} \tag{3f}$$

$$K(f_B, r) \le 0. \quad \text{(vehicle's passenger-carrying capacity constraint on boundary route)} \tag{3g}$$

2.4. Solution Procedures

For both models, we find a feasible (near-optimum) solution, and then compare the near optimum cost with a lower bound to comfirm the quality of the feasible solution. We will consider Model 1 first and then Model 2.

To construct a feasible solution for Model 1, fix the global variables $G = \{r; Q; f_B; f_G = \emptyset\}$ and consider the subproblem for the remaining decision function, $D(x)$. This problem only involves location-dependent constraints (3c, 3e, and 3f) unless $x = r$. The objective function is still (2) but the first term is fixed. The optimal decision function for the subproblem only depends on Q and for this reason will be denoted $D^o(x|Q)$. This subproblem can be seen to be a calculus of variations problem that further decomposes by x. In other words, for every x, $D^o(x|Q)$ is simply the value of D that minimizes the integrand portion of (2) subject to constraints (3c, 3e and 3f):

$$D^o(x|Q) = \text{argmin}_D\{\textstyle\sum_i z_i(D, r, x) : \ C(D, x, Q) = 0; \ K(D, x) \le 0\}, \ \ \forall x. \tag{4}$$

Because the optimization problem in (4) is not convex, we solve it numerically. For each instance of the problem, a search method was used ten times with ten randomly selected initial points to identify ten local optima. The least cost optimum was then identified as a candidate solution. This process was then repeated 15 times with different 10-point random samples of initial points to identify fifteen candidate solutions. In every instance of the problem we solved, the fifteen candidates coincided. This strongly suggests that these candidates are the globally optimal solutions (except when $x = r$) and that a single ten-point sample suffices to identify each globally optimal solution.

[8] This can be seen from (1), which implies: $\frac{2\pi x}{s_r(x)H_r(x)} - Q = 0$ for Model 1 and $\frac{8x}{s_r(x)H_r(x)} - Q = 0$ for Model 2.

To finish the process, now solve problem (2) and (3) with $D(x)$ replaced by $D^o(x|Q)$ (even when $x = r$) in order to identify $G^o = \{Q^o, r^o, f_B^o, F_G^o = \emptyset\}$. This is slightly suboptimal because $D^o(r|Q)$ is suboptimal. The numerical solution is simple because the problem is now an ordinary minimization problem with only four variables and a simple structure.[9] The final result, $\{G^o, D^o(x|Q^o)\}$, is the sought-after, near-optimum feasible solution. Since the solution is feasible, it is a upper bound to the exact optimum.

For the lower bound, we find the optimum of problem (2), (3) after relaxing constraints (3a) and (3b). Conditional on r and Q the relaxed problem now decomposes perfectly into two subproblems for the two sets of variables: G and $D(x)$. The subproblem for the second set $D(x)$ involves, as before, the second term of the objective function and location-dependent constraints (3c, 3e, and 3f), and its solution is the same as before. The subproblem for the first set $\{f_B; f_G = \emptyset\}$, involves the first term of the objective function and the remaning constraint (3g). This problem is simple as it only involves two variables. To find the unconditional optimum across all r and Q, which identify the lower bound, we look for the r and Q that minimize the sum of the costs of the two subproblems. As before, we find the solution by searching from numerous initial points.

For Model 2, all the processes are the same except that location-dependent constraints are now (3c, 3f).

To confirm the quality of the feasible solutions for both Model 1 and 2, we compared the cost of each feasible solution with its corresponding lower bound for each of 81 scenarios involving a wide variety of conditions; see Sec. 3[10]. In every case, the difference between the two costs for the ring-radial network averaged less than 1.5%, and it never exceeded 3.4%. For the grid network, the average difference was less than 1%. This confirms that the feasible solutions, found in the above way are indeed near-optimal.

3. Design: System Structure Insights

The procedures of Section 2.3 are now used to design systems for 81 different scenarios and to look for general insights. Section 3.1 examines Model 1 and Sec. 3.2 Model 2.

The scenarios in question will also be used in Secs. 4 and 5. The scenarios are constructed by changing the values of the three parameters that are most likely to differ greatly across cities: the city's surface area S $(50, 225, 400\ \text{km}^2)$; the demand density ρ $(50, 200, 600$ trips/h/km$^2)$; and the value of time μ $(5, 20, 50$ \$/h). In addition, three different transit modes are considered: Bus, BRT and Metro. Thus, there are 81 scenarios in total. The remaining parameters, which characterize the transit modes, are taken from Daganzo (2010)[11]. They are summarized in Table 1.

Table 1. Technology parameters for the considered scenarios.

Mode	$\$_L$ (\$/km-h)	$\$_V$ (\$/veh-km)	$\$_M$ (\$/veh-h)	$v(km/h)$	τ (sec/stop)	τ' (sec/p)	w (km/h)	C_{pax} (pax/veh)
Bus	9	2	40	25	30	1	2	120
BRT	90	2	40	40	30	1	2	150
Metro	900	6	120	60	45	$0^\dagger$	2	1200

†Zero is used because the vehicle's fixed dwell time is already sufficiently long to accomodate boardings.

The BRT scenario with $S = 225$ km^2, $\rho = 200$ trips/h/km^2, and $\mu = 20$ \$/h will be used as the base case for illustration purposes. We will find that the near-optimal configurations of Model 1 and Model 2 are quite different. This happens because the demand for travel, i.e. the spatial distribution of the passenger-miles traveled per unit time in different parts of a city, is very different for our two city types. Figure 3 shows the distribution of travel along rings as a function of x/R. Strikingly different among the two cities is the demand for travel along a ring for $x \approx R$, which reaches a minimum at $x = R$ for the circular city and a maximum for the square city. This difference in demand has a profound impact on the structures of the transit systems designed to accomodate it as we shall now see.

[9] Since constraints (3c-3f) are now redundant, the remaining relevant constraints and the objective function, can be seen to decompose into two independent subproblems: one for Q and the second for (r, f_B, f_G)

[10] The search process can be completed in less than 1 sec for each case.

[11] The values of τ' assume that fares are collected offline, see Daganzo (2010).

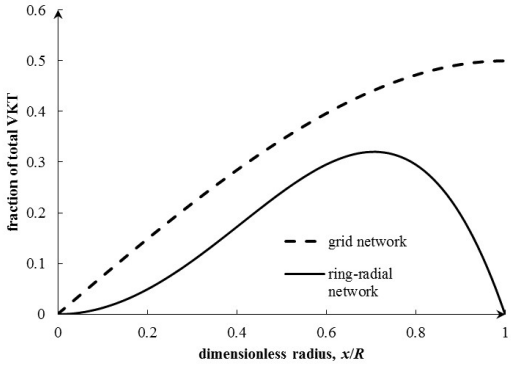

Fig. 3. Fraction of total vehicle kms flowing along a circular (square) crown of unit width and radius x/R

3.1. Optimum System Structure: Model 1

Figure 4a shows the main design variables obtained with the procedure of Sec. 2.4 for the base case scenario. Note how the ideal headways and spacings vary with distance from the city center even though travel demand is uniformly distributed. (Optimal designs would, of course, still feature spatial variations in headways and spacings in cases where demand varies with distance from the city center.) Figure 4b presents part of a network designed to have features similar to the ideal of Fig. 4a. In this figure, the thickness of each line represents its vehicle flows, with thicker lines denoting higher flows (lower headways).

Application of Model 1 to other scenarios involving ring-radial street networks produces outcomes that are similar to the ones in Fig. 4 Those results can be found in Chen, et al. (2014). The following discusses those features of Fig. 4 that apply to all the scenarios studied and can therefore be considered general.

Radial routes in the central district: The spacing of radial routes increases with x inside the central district; e.g., as shown by the solid curve in Fig. 4a for $0 < x < r \approx 3.07$ km in the base case. The rate of increase is only modest, however, so the radial routes need to bifurcate to match the ideal spacings approximately; e.g., as shown in Fig. 4b. The headways on these lines should grow with x as well, e.g. as shown by the bold dashed line of Fig. 4a for the base case. This growth is to be expected from the vehicle conservation rule (1), since at every bifurcation outbound transit vehicles diverge, thereby increasing the headway along the branching routes.

Circular routes in the central district: The spacing of the circular ring lines diminishes with x inside the central district. This is shown by the solid, thin curve in Fig. 4a for the base case. This occurs because with a ring-radial network the passenger demand for using the rings increases with x near the city center, see Fig 3. On the other hand, and like their radial counterparts, headways on the circular rings (dashed, thin curve) grow with x.

Size of the central district: Just as very few origin-destination pairs benefit from rings at $x \approx 0$, very few origin-destination pairs would use rings around $x \approx R$, see Fig 3. For this reason, circular routes with larger radii serve little purpose and should not be provided. As a result, the central districts in all cases studied turn out to be fairly small, with r/R rarely exceeding 50% – this ratio is 36% in Fig. 4a, so the central district covers only 13.1% of the area.

Radial routes at the boundary and in the periphery: In all cases studied the spacing between radial lines declines discontinuously at the boundary of the central district where $x = r$. See the jump in the bold solid line of Fig. 4a for the base case. This discontinuity is accommodated in actual plans by bifurcating the radial lines at the edge of the central district, e.g. as shown in Fig. 4b. Concurrent with this jump there must be in all cases a sudden increase in radial-line headways at $x = r$, as required by the vehicle conservation rule (1). This jump can also be seen in Fig. 4a. Finally, in the periphery itself, the radial routes turn out in all cases to be more closely spaced on average than in the central district, even though the spacing always increases slightly with x. Figure 4a illustrates the effect for the base case. The just discussed differences between radial service in the periphery and the central district are partly due to the lack of supporting ring routes in the periphery.

Circulator route on the boundary: In all cases studied, the service frequency on this route is considerably higher than on neighboring ring routes. For the base case this is shown by the black square in Fig. 3a, which is significantly below the thin dashed line. This happens because as Fig. 3 suggests the boundary route attracts a great deal of demand.

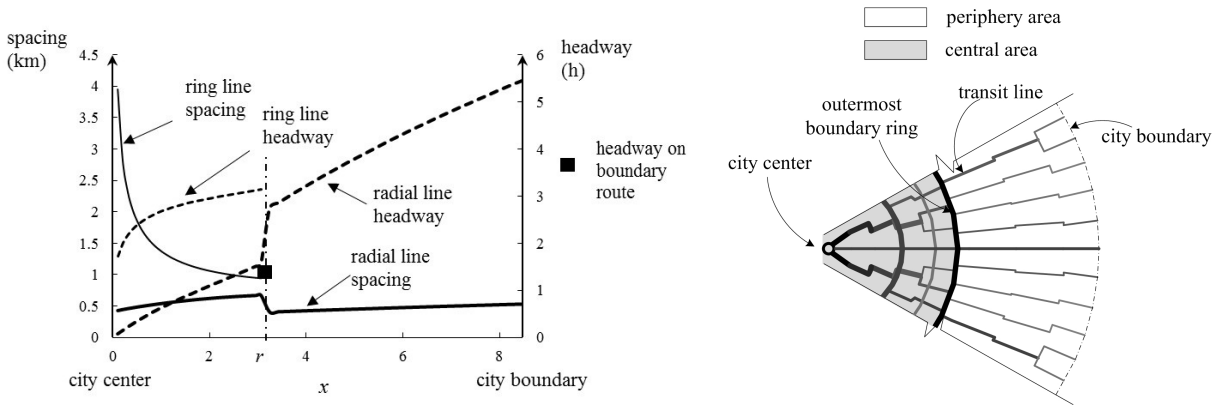

(a) Ideal features of an optimum ring-radial network

(b) Actual network with features resembling the idea

Fig. 4. Ring-radial network example for $S = 225$ km^2

3.2. Optimum System Structure: Model 2

Outcomes from the application of Model 2 to our base case scenario are displayed in Figs. 5a and b. Application of Model 2 to the other 80 scenarios produces similar outcomes; see Chen, et al. (2014). All the cases exhibit the following common features.

Size of the central district: The travel concentration phenomenon arising in the middle rings of ring-radial networks does not occur with street grids because these networks spread passenger traffic more evenly in space, see Fig 3. As a result, Model 2 always exhibits a much larger central district than Model 1 for the same parameter set. For example, for the base case scenario shown in Fig. 5, the central district is about four times larger than for Model 1, extending now to $x/R = r/R \approx 93\%$, and covering 87% of the area.

Routes in the central district and circulator on its boundary: By construction, all the routes in the interior of the central district have fixed headway and spacing. This is shown by the horizontal lines of Fig. 5a and the even grid of Fig. 5b. On the boundary, fewer passengers transfer than on the boundary of Model 1 because the periphery is now much smaller. As a result, it is never necessary to provide extra circulator buses to accommodate the extra transfers on these routes. It is found that in all cases studied it is optimal to set $H_B = H_g$. This feature is highlighted for the base case by the black square of Fig 5a, which lies on top of the grid line headway.

Radial routes at the boundary and in the periphery: As regards the radial routes in the periphery, and as illustrated for the base case by the slanted lines of Fig. 5a, the effects are similar to those of Model 1: (i) radial spacings that abruptly diminish at r to compensate for the abrupt discontinuation of double-coverage service; (ii) radial headways that abruptly expand at that location as outbound vehicles distribute themselves across branching routes; and (iii) headways and spacings that expand gradually as the routes approach the city boundary.

4. Comparisons

This section applies the models to the 81 cases from Section 3. Sect 4.1 compares the costs between circular and grid cites. Sect 4.2 discusses the robustness of the models by comparing the predicted optimum cost with the cost arising when the optimum decision variables are used to design a transit system on the other city type (grid for Model 1 and ring-radial for Model 2). Finally, Sect 4.3 compares the cost between CA and non-CA models.

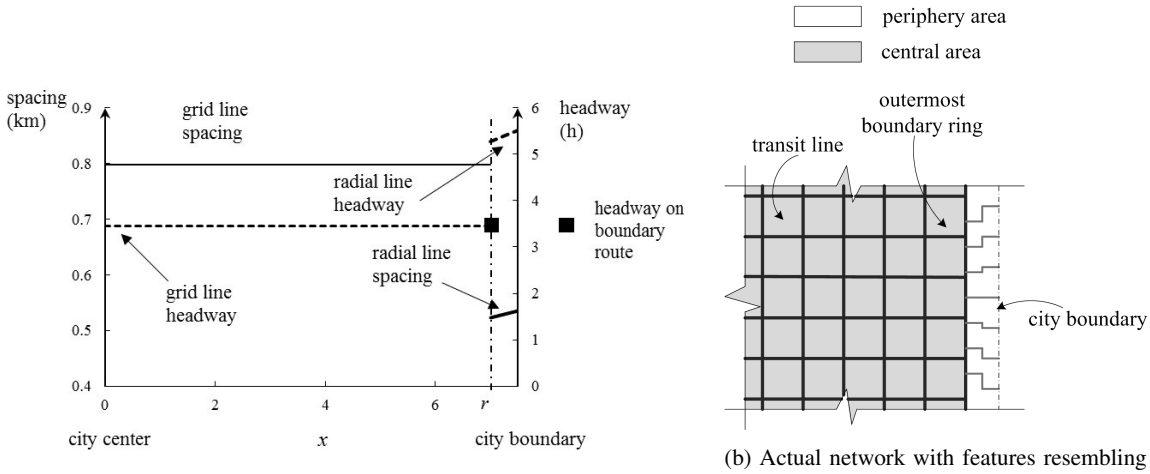

(a) Ideal features of an optimum grid network

(b) Actual network with features resembling the idea

Fig. 5. Grid network example for $S = 225$ km^2

4.1. Comparisons between ring-radial and grid cities

Costs are now compared. For ease of interpretation we will use average unit costs (per trip) rather than total cost. Furthermore, to be currency-independent, we shall use as the monetary unit the amount of money equivalent to one hour of travel.

Figure 6 compares the optimum costs of Models 1 and 2 for the 81 cases.[12] Note how the ring-radial networks always result in lower generalized costs. Differences in the costs of the two structures are typically between 9% and 13%, though differences as high as 21.5% are also observed. The finding means that the ring-radial street layouts are always more transit-friendly than grids. This happens for two reasons. First, ring-radial networks allow for more direct travel than do grids; e.g. see Fairthorne (1963). And second, because ring-radial networks tend to concentrate travel demand on certain rings (see Fig. 3), which is a good thing for collective transportation because it, unlike automobile travel, becomes more efficient when traffic is spatiotemporally concentrated (e.g. see Daganzo 2010a).

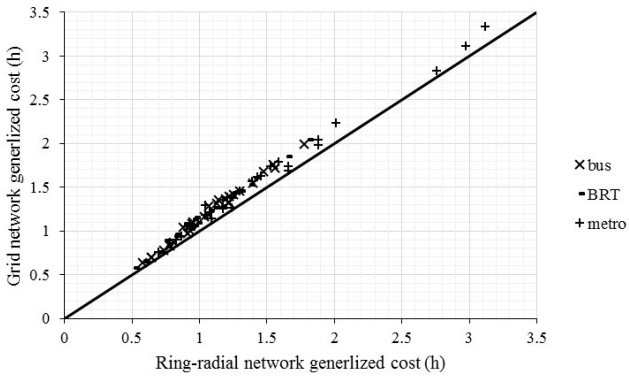

Fig. 6. Parametric comparisons

[12] Numerical results are tabulated in Chen, et al. (2014)

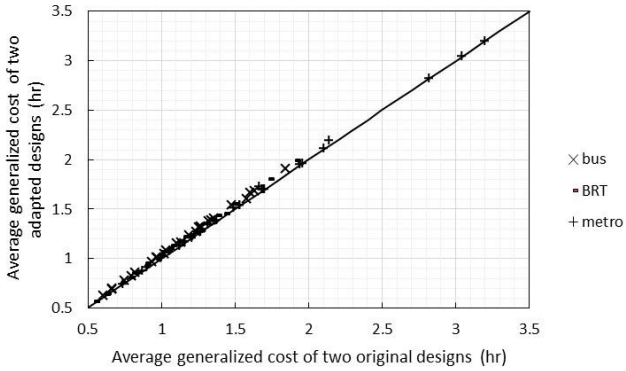

Fig. 7. Tests of model robustness

4.2. Model robustness

As in Estrada, et al. (2011) we now examine the suitability of the two CA models for designing transit routes to fit over city-street networks that are different from what the models assume. This is again done using the same 81 cases of Section 3. For each case, each hybrid ring-radial transit design was adapted to conform to a grid street network, and each hybrid grid transit design was adapted to a ring-radial street network.[13] The costs of the adapted and original designs were then compared.

Robustness is revealed by seeing how the costs for a given transit morphology change when the design is adapted. Curiously, it is found that the costs of hybrid grid transit systems always decline slightly (by 1-2%) when they are adapted to sit on ring radial street networks, but the reverse is not true. This happens partly because the origins and destinations of circular cities with ring-radial street networks are closer to one another than those of square cities with street grids, so that any adaptation to ring-radial streets helps reduce the average user distance traveled.

In order to exclude these structural effects from our robustness tests we compared the average costs of the two adapted designs with the average of the two originals. Figure 7 displays the results. As expected, controlling for city structure, the adaptations add to the costs, but only slightly – 2.7% on average. So the CA method appears to be robust. The differences between a real street network and the best-matching idealized street network (grid or radial) are likely to be smaller than the differences underlying Fig 7. This means that if one fits a hybrid grid transit system to a street network roughly resembling a grid, or a ring-radial system to a street network with an approximate ring-radial structure the model prediction errors should be smaller than those of Fig. 7.

4.3. Comparions between CA and non-CA models

The costs arising with the two CA models are now compared against the costs produced by comparable non-CA models with three variables (r, s_g, H_g).[14] The results illustrate that the average cost of the CA models is 3.11% lower than that of the non-CA models for Model 1 and 3.35% for Model 2. This comparison reveals that the benefits of spatial variations in headways and spacings is significant but limited. We expect similar benefits to hold when the models are applied in reality because our tests show that the non-CA models are not more robust than the CA models.[15] It thus appears that the first order of business when desiging a transit system is to get the line spacings, headways and central district sizes right.

[13] In each case, the design variables from Model 1(2) were chosen to match the optima generated from Model 2(1). These design variables were redefined so that they would apply to both city-street structures. These variables were the: transit networks total length; total vehicle distance traveled each hour; and area of the central district. These three variables co-determine the transit networks spatial layout and determine the headways.

[14] The non-CA models assume that the line spacing and headway (i.e., s_c, H_c, and s_r for model 1 and s_r for model 2) are homogeneous over the entire city.

[15] Cost increases by about 6% on average when a non-CA model is fit to the ”wrong” city.

5. Conclusions

The two models presented in this paper use CA methods to fit transit systems atop a city's streets so as to minimize the generalized cost of a trip. The methods lend themselves nicely to the design of systems with vehicle headways and line spacings that can vary with location in the city, so as to better serve its travel demand. Model 1 was formulated for cities with ring-radial street networks. It allows spacings and headways to vary optimally over an entire city, and extends the model in Vaughan (1986) by allowing for a hybrid structure of transit lines. Moreover, Model 1 repairs the flaws of Vaughan's model by constraining the tours of radial-line vehicles. Model 2 was developed for cities with grid-street networks. It generalizes Daganzo (2010) by allowing headways and spacings to vary within a city's periphery.

Application of the models to a wide range of scenarios reveals that Model 1 always has a lower cost than Model 2 on comparable cities. This suggests that ring-radial networks are considerately more friendly to transit than are grids. It was also found that the CA models improve cost, albert only by about 3%, with non-CA counterparts. Robustness tests suggest that the CA models can be used confidently on cities that have networks resembling the ideal, and that the benefits of the CA models continue to hold when the models are applied to real networks.

Acknowledgements

Research supported by NSF GRANT–CMMI-1161427.

Appendix A. Model 1 for ring-radial networks

We derive each of the components for Model 1. The notation is as follows.

Nomenclature

r	Radius of the city's central district
R	Radius of the city boundary
x	Distance to the city center
θ	Angle between the origin and destination in polar coordinates centered at the city center
Λ	Travel demand for the entire city (p/h) in the rush hour
τ	Vehicle lost time at each station due to acceleration and deceleration
τ'	Boarding time per passenger
C_{pax}	Vehicle passenger-carrying capacity
s	Station spacing throughout the city
v_B	cruising speed on the outermost (boundary) ring line
$s_c(x)$	Ring line spacing at distance x
$s_r(x)$	Radial line spacing at x
$v_{cc}(x)$	Commercial speed on ring line at x
$v_{cr}(x)$	Commercial speed on radial line at x
$v_c(x)$	Cruising speed on ring line at x
$v_r(x)$	Cruising speed on radial line at x
$H_c(x)$	Headway on ring line at x
$H_r(x)$	Headway on radial line at x
$P_o(x)$	Probability that the origin lies within rings of radii $(x, x + dx)$
$P_d(x)$	Probability that the destination lies within rings of radii $(x, x + dx)$
$O(x)$	Maximum expected number of passengers in a vehicle serving the ring at x
Q	Total flow of radial-line buses across every ring

A.1. Local cost for the length of the transit lines: $y_L(x)$

Consider a pair of rings of radii $(x, x + dx)$. The area between those rings is $2\pi x dx$, and contains $\frac{2\pi x}{s_r(x)}$ radial lines, each of length dx. Therefore, the length of the network's radial lines within the ring pair is $\frac{2\pi x}{s_r(x)}dx$. The area similarly contains $\frac{dx}{s_c(x)}$ ring lines, each of length $2\pi x$. The length of the ring lines is therefore $\frac{2\pi x}{s_c(x)}dx$. The local cost of that length, $y_L(x)$, is the length of the transit lines in the area divided by the area's width dx; that is: $y_L(x) = \frac{2\pi x}{s_r(x)} + \frac{2\pi x}{s_c(x)}$ in the central district, and $\frac{2\pi x}{s_r(x)}$ in the periphery.

A.2. Local cost for the vehicle-distance traveled per hour: $y_V(x)$

Consider again the ring lines of area $2\pi x dx$. The $y_V(x)$ is obtained by multiplying the local cost of ring-line and radial-line distances, $\frac{2\pi x}{s_c(x)}$ and $\frac{2\pi x}{s_r(x)}$, with their corresponding transit flows, $\frac{1}{H_c(x)}$ and $\frac{1}{H_r(x)}$, and multiplying by the factor 2 to account for the bi-dierctional travel on each line. Thus, the local cost for the vehicle-distance traveled per hour $y_V(x)$ is: $\frac{4\pi x}{s_r(x)H_r(x)} + \frac{4\pi x}{s_c(x)H_c(x)}$ in the central district; and $\frac{4\pi x}{s_r(x)H_r(x)}$ in the periphery.

A.3. Global cost for the vehicle-distance traveled per hour: F_V

For the global cost, we consider only the cost on the outermost (boundary) ring line. Thus, the vehicle-distance traveled per hour on that ring is: $\frac{4\pi r}{H_B}$.

A.4. Local cost for the fleet size during the rush: $y_M(x)$

The $y_M(x)$ is obtained from the result of B.2 and the vehicles' commercial speed at distance x. Thus, $y_M(x)$ is: $\frac{4\pi x}{s_r(x)H_r(x)v_{cr}(x)} + \frac{4\pi x}{s_c(x)H_c(x)v_{cc}(x)}$ in the central district; and $\frac{4\pi x}{s_r(x)H_r(x)v_{cr}(x)}$ in the periphery.

A.5. Global cost for the fleet size during the rush: F_M

Much as in B.4, F_M is obtained from the result of B.3 and the vehicle's commercial speed at the outermost (boundary) ring. Thus, F_M is: $\frac{4\pi r}{H_B v_{cB}}$.

A.6. Local cost for the patron's average waiting time: $y_W(x)$

We divide the problem into six cases, as shown in Fig. B8. For the first case, the trip's origin and destination both lie in the periphery and $\theta < 2$, see case 1 in the figure. In this case, a patron takes a radial line, transfers at the outermost ring and transfers again to another radial line to reach her destination. The patron would thus encounter an expected waiting time $\left(\frac{H_r(x)}{2} + \frac{H_r(y)}{2}\right)$ at radial-line stations. For calculating local cost, we do not consider the waiting time at the outermost ring (This is part of the global cost). The local cost for this case is therefore: $(P_o(x)\int_r^R P_d(y)dy + P_d(x)\int_r^R P_o(y)dy)\frac{2}{\pi}\frac{H_r(x)}{2}$ for $r < x < R$.

For the second case, the origin and destination again lie in the periphery, but $\theta > 2$, see case 2 in Fig. B8. The patron in this case travels by two radial lines and transfers at the city center as shown in the figure, such that the local cost for the waiting time is: $(P_o(x)\int_r^R P_d(y)dy + P_d(x)\int_r^R P_o(y)dy)(1 - \frac{2}{\pi})\frac{H_r(x)}{2}$ for $r < x < R$.

For the third case, the origin and destination both lie in the central district (i.e. $0 < x < r$) and $\theta < 2$; see case 3 in Fig. B8. The patron travels by ring and radial lines. Her local cost for waiting time is: $\frac{H_c(x)}{2}P_o(x)\frac{2}{\pi}\int_x^r P_d(y)dy + \frac{H_r(x)}{2}P_d(x)\frac{2}{\pi}\int_x^r P_o(y)dy$ if $x < y$ and $\frac{H_c(x)}{2}P_d(x)\frac{2}{\pi}\int_x^r P_o(y)dy + \frac{H_r(x)}{2}P_o(x)\frac{2}{\pi}\int_x^r P_d(y)dy)$ otherwise.

The fourth case is like the third, except that $\theta > 2$; see case 4 in Fig. B8. The local cost for this case is: $(P_o(x)dx\int_0^r P_d(y)dy + P_d(x)\int_0^r P_o(y)dy)(1 - \frac{2}{\pi})\frac{H_r(x)}{2}$ for $0 < x < r$.

For the fifth case, the origin is in the central district, the destination is in the periphery (or vise versa), and $\theta < 2$, see case 5 in Fig. B8. The local costs for waiting time are: $(P_d(x)\int_0^r P_o(y)dy + P_o(x)\int_0^r P_d(y)dy)\frac{2}{\pi}\frac{H_r(x)}{2}$ for $r < x < R$; and $(P_o(x)\int_r^R P_d(y)dy + P_d(x)\int_r^R P_o(y)dy)\frac{2}{\pi}\frac{H_c(x)}{2}$ for $0 < x < r$.

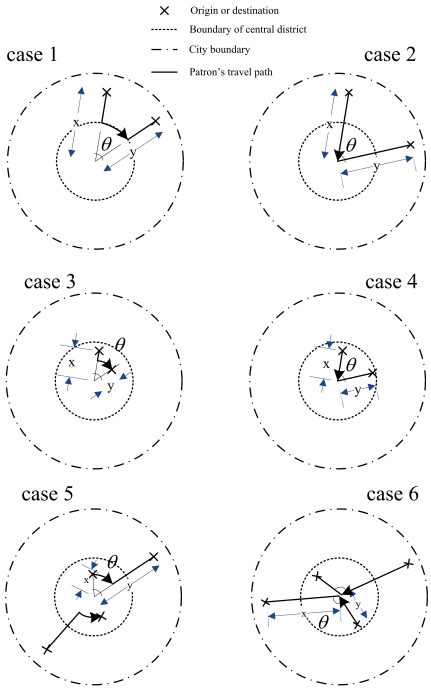

Fig. A.8. cases for average waiting time per trip

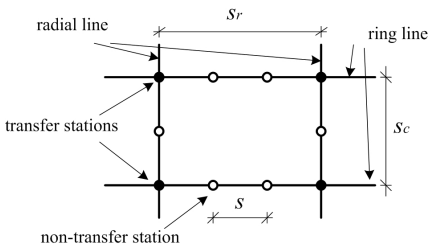

Fig. A.9. transit stations in the central district

The sixth case is like the fifth, except that $\theta > 2$; see case 6 in Fig. B8. The local costs for waiting time are: $(P_d(x)\int_0^r P_o(y)dy + P_o(x)\int_0^r P_d(y)dy)\left(1-\frac{2}{\pi}\right)\frac{H_r(x)}{2}$ for $r < x < R$; and $(P_d(x)\int_r^R P_o(y)dy + P_o(x)\int_r^R P_d(y)dy)\left(1-\frac{2}{\pi}\right)\frac{H_r(x)}{2}$ for $0 < x < r$.

The sum of the six cases above is the local cost for the waiting time per trip $y_W(x)$: $\frac{H_c(x)}{\pi}P_o(x)\left(\int_x^R P_d(y)dy\right) + \frac{H_c(x)}{\pi}P_d(x)\left(\int_x^R P_o(y)dy\right) + \frac{H_r(x)}{\pi}P_o(x)\left(\int_0^x P_d(y)dy\right) + \frac{H_r(x)}{\pi}P_d(x)\left(\int_0^x P_o(y)dy\right) + \frac{H_r(x)}{2}\left(1-\frac{2}{\pi}\right)P_o(x) + \frac{H_r(x)}{2}\left(1-\frac{2}{\pi}\right)P_d(x)$ for $0 < x < r$; and $\frac{H_r(x)}{2}(P_o(x) + P_d(x))$ for $r < x < R$.

A.7. Global cost for the patron's average waiting time: F_W

For global cost, we only consider the cost happened at the outermost ring line. Thus, the trip's origin and destination both lie in the periphery area and $\theta < 2$. and the waiting time at the outermost ring line (i.e. F_W) is: $\int_r^R P_o(x)dx \int_r^R P_d(y)\frac{2}{\pi}\frac{H_B}{2}$

A.8. Local cost for access time: $y_A(x)$

Transfer stations reside at all intersections of ring and radial lines, and intermediate, non-transfer stations are spaced at s over the network; see Fig. B9. We use $\frac{ss_r}{s+s_r}$ as the average station spacing along the rings, and $\frac{ss_c}{s+s_c}$ along the radials. These continuum approximations are reasonable when s_c and s_r are both larger than s. Thus, a patron who originates within a central district is expected to travel distance $\frac{1}{4}\left(s_r + \frac{ss_c}{s+s_c}\right)$ to access a ring line, and distance $\frac{1}{4}\left(s_c + \frac{ss_r}{s+s_r}\right)$ to access a radial line. Average walking distance is $\frac{1}{4}(s_r + s)$ in the periphery.

We divide the problem into six cases, as shown in Fig. B10. In the first case: the trip's origin and destination both lie in the central district; the origin lies closer to the city center than does the destination; and $\theta < 2$; see case 1 in the figure. A patron takes a ring line, and transfers to a radial line to reach her destination. The access time from her origin to the nearest station on the ring line is: $\frac{1}{w}\left(\frac{1}{4}\frac{ss_r(x)}{s+s_r(x)} + \frac{1}{4}s_c(x)\right)$, and the access time from the nearest stop on the radial line to the destination is: $\frac{1}{w}\left(\frac{1}{4}\frac{ss_c(x)}{s+s_c(x)} + \frac{1}{4}s_r(x)\right)$. The local cost for this case is therefore: $P_o(x)\int_x^r P_d(y)\frac{2}{\pi w}\left(\frac{1}{4}\frac{ss_r(x)}{s+s_r(x)} + \frac{1}{4}s_c(x)\right)dy + P_d(x)\int_0^x P_o(y)\frac{2}{\pi w}\left(\frac{1}{4}\frac{ss_c(x)}{s+s_c(x)} + \frac{1}{4}s_r(x)\right)dy$ for $0 < x < r$.

The second case is like the first, except that the destination is closer to the city center than is the origin; see case 2 in Fig. B10. The local cost for this case is: $P_o(x)\int_0^x P_d(y)\frac{2}{\pi w}\left(\frac{1}{4}\frac{ss_c(x)}{s+s_c(x)} + \frac{1}{4}s_r(x)\right)dy + P_d(x)\int_x^r P_o(y)\frac{2}{\pi w}(\frac{1}{4}\frac{ss_r(x)}{s+s_r(x)} + \frac{1}{4}s_c(x))dy$ for $0 < x < r$.

For the third case, the origin and destination again lie in the central district, but $\theta > 2$; see case 3 in Fig. B10. The patron in this case, travels by two radial lines as shown in the figure, such that the local cost for access time is: $P_o(x)\int_0^r P_d(y)\left(1-\frac{2}{\pi}\right)\frac{1}{w}\left(\frac{1}{4}\frac{ss_c(x)}{s+s_c(x)} + \frac{1}{4}s_r(x)\right)dy + P_d(x)\int_0^r P_o(y)\left(1-\frac{2}{\pi}\right)\frac{1}{w}\left(\frac{1}{4}\frac{ss_c(x)}{s+s_c(x)} + \frac{1}{4}s_r(x)\right)dy$ for $0 < x < r$, where the first term is the expected access time from the origin (located at x) to the radial line, and the second term is the expected access time from the radial line to the destination.

For the fourth case, the origin is in central district, the destination is in the periphery (or vice-versa), and $\theta < 2$; see case 4 in Fig. B10. The patron in this case travels along the ring line, and transfers to the radial line that leads to her the destination. The local cost for access time at the origin (or destination) is therefore either: $P_o(x)\int_r^R P_d(y)dy\left[\frac{2}{\pi w}(\frac{1}{4}\frac{ss_r(x)}{s+s_r(x)} + \frac{1}{4}s_c(x))\right]$, or $P_d(x)\int_r^R P_o(y)dy\left[\frac{2}{\pi w}\left(\frac{1}{4}\frac{ss_r(x)}{s+s_r(x)} + \frac{1}{4}s_c(x)\right)\right]$, for $0 < x < r$.

The fifth case is like the fourth, except that $\theta > 2$; see case 5 in Fig. B10. This patron travels only by radial lines, and the local cost for access time in the central district is: $\left(P_d(x)\int_r^R P_o(y)dy + P_o(x)\int_r^R P_d(y)dy\right)\left[(1-\frac{2}{\pi})\frac{1}{w}(\frac{1}{4}\frac{ss_c(x)}{s+s_c(x)} + \frac{1}{4}s_r(x))\right]$ for $0 < x < r$.

For convenience, the access times that occur in the peripheries were thus far ignored for cases 4 and 5. Those peripheral access times are instead accounted for in the sixth case; see case 6 in Fig. B10. The local cost is $(P_o(x) + P_d(x))\left(\frac{1}{4}s_r(x) + \frac{1}{4}s\right)\frac{1}{w}$ for $r < x < R$.

The sum of the six cases above is the entire local cost for access time, $y_A(x)$: $P_o(x)\int_x^r P_d(y)\frac{2}{\pi w}\left(\frac{1}{4}\frac{ss_r(x)}{s+s_r(x)} + \frac{1}{4}s_c(x)\right)dy + P_o(x)\int_0^x P_d(y)\frac{2}{\pi w}\left(\frac{1}{4}\frac{ss_c(x)}{s+s_c(x)} + \frac{1}{4}s_r(x)\right)dy + P_d(x)\int_x^r P_o(y)\frac{2}{\pi w}\left(\frac{1}{4}\frac{ss_r(x)}{s+s_r(x)} + \frac{1}{4}s_c(x)\right)dy + P_d(x)\int_0^x P_o(y)\frac{2}{\pi w}\left(\frac{1}{4}\frac{ss_c(x)}{s+s_c(x)} + \frac{1}{4}s_r(x)\right)dy + P_o(x)\int_0^r P_d(y)\left(1-\frac{2}{\pi}\right)\frac{1}{w}\left(\frac{1}{4}\frac{ss_c(x)}{s+s_c(x)} + \frac{1}{4}s_r(x)\right)dy + P_d(x)\int_0^r P_o(y)\left(1-\frac{2}{\pi}\right)\frac{1}{w}\left(\frac{1}{4}\frac{ss_c(x)}{s+s_c(x)} + \frac{1}{4}s_r(x)\right)dy + (P_d(x)\int_r^R P_o(y)dy + P_o(x)\int_r^R P_d(y)dy)\left[\frac{2}{\pi w}\left(\frac{1}{4}\frac{ss_r(x)}{s+s_r(x)} + \frac{1}{4}s_c(x)\right) + \left(1-\frac{2}{\pi}\right)\frac{1}{w}\left(\frac{1}{4}\frac{ss_c(x)}{s+s_c(x)} + \frac{1}{4}s_r(x)\right)\right]$ for $0 < x < r$; and $(P_o(x) + P_d(x))(\frac{1}{4}s_r(x) + \frac{1}{4}s)\frac{1}{w}$, for $r < x < R$.

A.9. Ring-line commercial speed: $v_{cc}(x) = 1/(\frac{1}{v_c(x)} + \tau(\frac{1}{s} + \frac{1}{s_r(x)}) + \tau'\Lambda[P_o(x)\int_x^R P_d(y)dy + P_d(x)\int_x^R P_o(y)dy]\frac{s_c(x)H_c(x)}{2\pi^2 x})$

The commercial speed in the central district, $v_{cc}(x)$, is determined by: 1) the cruising time per unit distance, $\frac{1}{v_c(x)}$; 2) the time lost at stations per unit distance due to acceleration and deceleration, $\tau(\frac{1}{s} + \frac{1}{s_r(x)})$; and 3) the time spent boarding patrons per unit distance, $\tau'\Lambda[P_o(x)\int_x^R P_d(y)dy + P_d(x)\int_x^R P_o(y)dy]\frac{s_c(x)H_c(x)}{2\pi^2 x}$.

When calculating commercial speed (as well as the maximum expected number of passengers in a vehicle), the travel demand during the rush, Λ, is used to account for the worst case condition. We fix Λ to be 2.5 times the average day-long travel demand.

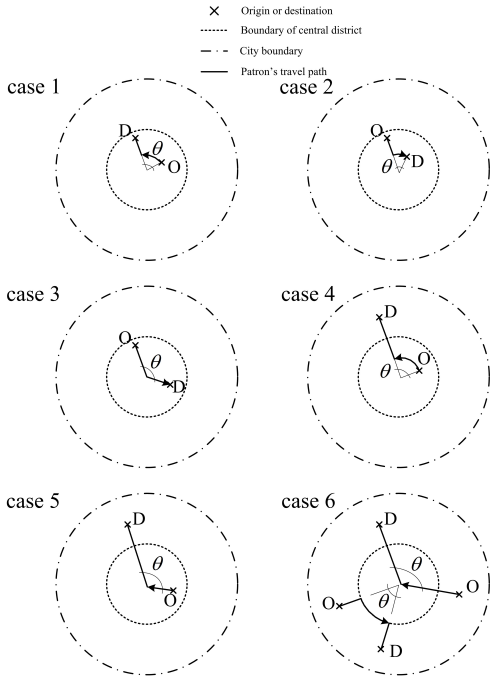

Fig. A.10. Cases for average access time per trip

A.10. Radial-line commercial speed: $v_{cr}(x)$

Since the average station spacings are different for the central district than for the periphery, the radial-line commercial speeds have different expressions. In the central district, we have: $v_{cr}(x) = 1/(\frac{1}{v_r(x)} + \tau(\frac{1}{s} + \frac{1}{s_c(x)}) + \tau' \frac{\Lambda P_o(x) s_r(x) H_r(x)}{4\pi x})$. In the periphery: $v_{cr}(x) = 1/(\frac{1}{v_r(x)} + \tau(\frac{1}{s}) + \tau' \frac{\Lambda P_o(x) s_r(x) H_r(x)}{4\pi x})$. The speed has three components: 1) cruising time, $\frac{1}{v_r(x)}$; 2) lost time at transit stations, $\tau(\frac{1}{s} + \frac{1}{s_c(x)})$ (or $\tau(\frac{1}{s})$); and 3) passenger boarding time, $\tau' \frac{\Lambda P_o(x) s_r(x) H_r(x)}{4\pi x}$.

A.11. Commercial speed on outermost boundary ring: $v_{cB} = 1/(\frac{1}{v_B} + \tau(\frac{1}{s} + \frac{1}{s_r(r)}) + \tau'\Lambda[\int_r^R P_o(y)dy \int_r^R P_d(y)dy]\frac{H_B}{2\pi^2 r})$

Much as in B.9 and B.10, the commercial speed on the boundary route has three components: 1) cruising time, $\frac{1}{v_B}$; 2) lost time at transit stations, $\tau(\frac{1}{s} + \frac{1}{s_r(r)})$; and 3) passenger boarding time, $\tau'\Lambda[\int_r^R P_o(y)dy \int_r^R P_d(y)dy]\frac{H_B}{2\pi^2 r})$.

A.12. Local cost for expected in-vehicle travel time: $y_T(x)$

Consider a pair of rings of radii $(x, x+dx)$, as shown by the grey-shaded swath in Fig. B11. We obtain the in-vehicle travel time on that swath weighted by the proportion of patrons who travel along it and who cross it. We do this for the swaths at each $x < R$, and divide the in-vehicle travel time on that swath by the width of the swath, dx, to obtain $z_T(x)$. We do not consider the in-vehicle travel time on the outermost boundary ring line here. It is instead included in the global cost for in-vehicle travel time, F_T.

The problem is divided into three cases. The first of these pertains to patrons who use only radial lines (i.e. $\theta > 2$), as exemplified in Fig. B11. Note from the two example trips in that figure how patrons might cross a swath once or twice. The time spent crossing a swath at distance x is $\frac{dx}{v_{cr}(x)}$. Multiplying by the proportion of patrons who make the trip, we obtain: $(1-\frac{2}{\pi})[2\int_x^R P_o(y)dy \int_x^R P_d(y)dy + \int_x^R P_o(y)dy \int_0^x P_d(y)dy + \int_x^R P_d(y)dy \int_0^x P_o(y)dy]\frac{1}{v_{cr}(x)}$ for $0 < x < R$.

The second case pertains to patrons who use radial lines and the outermost boundary ring, as shown in Fig. B12. Much as in the previous case, patrons on radial lines will cross ring-shaped swaths once or twice. Hence, the weighted

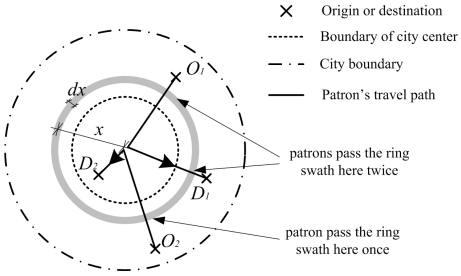

Fig. A.11. the fisrt case for expected in-vehicle travel time

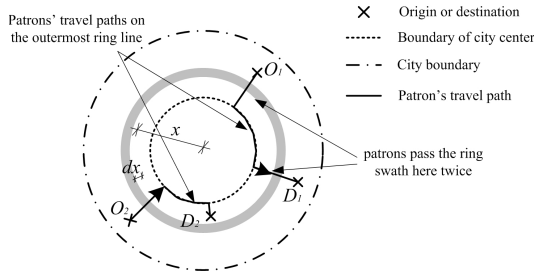

Fig. A.12. the second case for expected in-vehicle travel time

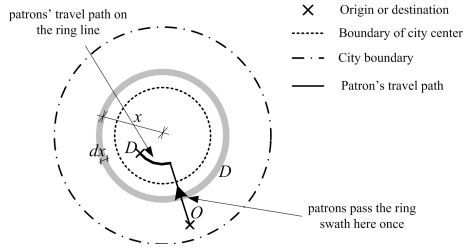

Fig. A.13. the third case for expected in-vehicle travel time

in-vehicle travel time spent at x except for the travel time on the boundary ring is: $\frac{2}{\pi}\int_x^R P_o(y)dy\int_x^R P_d(y)dy\frac{2}{v_{cr}(x)}$ + $\frac{2}{\pi}(\int_x^R P_o(y)dy\int_0^x P_d(y)dy+\int_x^R P_d(y)dy\int_0^x P_o(y)dy)\frac{1}{v_{cr}(x)}$ for $r < x < R$.

The third case pertains to patrons whose origins and/or whose destinations lie in the central district, as exemplified for one case in Fig. B13. The in-vehicle time spent on a ring at x is: $(P_d(x)\int_x^R P_o(y)dy)\frac{2x}{\pi}\frac{1}{v_{cc}(x)}$. These patrons cross a ring-shaped swath no more than once. Thus, the local cost for in-vehicle time for this case is: $(P_d(x)\int_x^R P_o(y)dy)\frac{2x}{\pi}\frac{1}{v_{cc}(x)}+\frac{2}{\pi}(\int_x^R P_o(y)dy\int_0^x P_d(y)dy+\int_x^R P_d(y)dy\int_0^x P_o(y)dy)\frac{1}{v_{cr}(x)}$ for $0 < x < r$.

The sum of the three cases is the local cost for expected in-vehicle travel time, $y_T(x)$: $(1-\frac{2}{\pi})[2\int_x^R P_o(y)dy\int_x^R P_d(y)dy+\int_x^R P_o(y)dy\int_0^x P_d(y)dy+\int_x^R P_d(y)dy\int_0^x P_o(y)dy]\frac{1}{v_{cr}(x)}+\frac{2}{\pi}\int_x^R P_o(y)dy\int_x^R P_d(y)dy\frac{2}{v_{cr}(x)}+\frac{2}{\pi}(\int_x^R P_o(y)dy\int_0^x P_d(y)dy+\int_x^R P_d(y)dy\int_0^x P_o(y)dy)\frac{1}{v_{cr}(x)}$, for $r < x < R$; and $(1-\frac{2}{\pi})[2\int_x^R P_o(y)dy\int_x^R P_d(y)dy+\int_x^R P_o(y)dy\int_0^x P_d(y)dy+\int_x^R P_d(y)dy\int_0^x P_o(y)dy]\frac{1}{v_{cr}(x)}+\frac{2}{\pi}(\int_x^R P_o(y)dy\int_0^x P_d(y)dy+\int_x^R P_d(y)dy\int_0^x P_o(y)dy)\frac{1}{v_{cr}(x)}+(P_o(x)\int_x^R P_d(y)dy+P_d(x)\int_x^R P_o(y)dy)\frac{2x}{\pi}\frac{1}{v_{cc}(x)}$ for $0 < x < r$.

A.13. Global cost for expected in-vehicle travel time: F_T

For global cost, we consider only the cost at the outermost boundary ring. Thus, the trip's origin and destination both lie in the periphery and $\theta < 2$. The in-vehicle travel time at the boundary ring, F_T, is: $\int_r^R P_o(x)dx\int_r^R P_d(x)dx\frac{2r}{\pi}\frac{1}{v_{cB}}$.

A.14. Global cost for expected number of transfers: $F_{e_T} = 1+\frac{2}{\pi}\int_r^R P_o(x)dy\int_r^R P_d(x)dy$

All patrons must transfer at least once each trip. Those whose origins and destinations both lie in the periphery must transfer twice, and the added expectation is given in the second term of the above expression.

A.15. Vehicles passenger-carrying capacity constraint except on boundary ring

The expected maximum number of patrons on board a vehicle should be constrained to be less than the vehicle's passenger-carrying capacity. The total number onboard all vehicles on a ring line at distance x is: $\Lambda(P_o(x)\int_x^R P_d(y)dy+P_d(x)\int_x^R P_o(y)dy)\frac{2}{\pi}$. The flow of transit vehicles on that ring is: $2/(s_c(x)H_c(x))$. And the ratio of the average trip

length to the length of the ring line is: $\frac{x}{2\pi x}$. Hence, the expected maximum on that ring line is: $\Lambda(P_o(x)\int_x^R P_d(y)dy + P_d(x)\int_x^R P_o(y)dy)\frac{2}{\pi}\frac{1}{2/(s_c(x)H_c(x))}\frac{x}{2\pi x}$.

In similar fashion, the expected maximum number onboard a radial line at x is: $\Lambda(\int_x^R P_o(d)dy\int_0^x P_d(y)dy\frac{2}{\pi} + \int_x^R P_o(y)dy(1-\frac{2}{\pi}))\frac{1}{2\pi x/(s_r(x)H_r(x))}$ in the inbound direction, and $\Lambda(\int_x^R P_d(d)dy\int_0^x P_o(y)dy\frac{2}{\pi}+\int_x^R P_d(y)dy(1-\frac{2}{\pi}))\frac{1}{2\pi x/(s_r(x)H_r(x))}$ outbound.

Thus, the maximum of expected number of passengers in a vehicle at x, $O(x)$, is: $\max[\Lambda(P_o(x)\int_x^R P_d(y)dy + P_d(x)\int_x^R P_o(y)dy)\frac{2}{\pi}\frac{1}{2/(s_c(x)H_c(x))}\frac{x}{2\pi x};\ \Lambda(\int_x^R P_o(d)dy\int_0^x P_d(y)dy\frac{2}{\pi} + \int_x^R P_o(y)dy(1-\frac{2}{\pi}))\frac{1}{2\pi x/(s_r(x)H_r(x))};\ \Lambda(\int_x^R P_d(d)dy\int_0^x P_o(y)dy\frac{2}{\pi} + \int_x^R P_d(y)dy(1-\frac{2}{\pi}))\frac{1}{2\pi x/(s_r(x)H_r(x))}]$. And the vehicle's passenger-carrying capacity constraint (except at the boundary ring) is: $O(x) - C_{pax} < 0$.

A.16. Vehicle's passenger-carrying capacity constraint on boundary ring

Much like in the A.15, the total number onboard all vehicles on the outermost boundary ring is: $\Lambda(\int_r^R P_o(y)dy\int_r^R P_d(y)dy)\frac{2}{\pi}$. The flow of transit vehicles on that ring is: $\frac{2}{H_B}$. And the ratio of the average trip length to the length of the ring line is: $\frac{1}{2\pi}$. Hence, the expected maximum number of passengers in a vehicle on the boundary ring, O_B, is: $\Lambda(\int_r^R P_o(y)dy\int_r^R P_d(y)dy)\frac{2}{\pi}\frac{H_B}{2}\frac{1}{2\pi}$. And the vehicle's passenger-carrying capacity constraint on that ring is: $O_B - C_{pax} < 0$.

A.17. Vehicle conservation for radial-line buses

The vehicle conservation constraints are derived from Equation (1) and the total flow of radial-line buses across every ring is obtained from the radial-line bus flow at the outmost ring, i.e. $Q = \frac{2\pi R}{s_r(R)H_r(R)}$. Thus, the vehicle conservation constraint for radial-line buses is: $Q = \frac{2\pi x}{s_r(x)H_r(x)}, \forall x \in [0, R]$.

Appendix B. Grid transit network model

We begin by introducing some new terms not used in Appendix B.

Nomenclature

α	Ratio of central district size to the city size, i.e. $\alpha = \frac{r}{R}$
s_g	Line spacing in the central district
v_{ci}	Commercial speed in the central district
v_g	Vehicle cruising speed in the central district
H_g	Headway in the central district

B.1. Local cost for length of the transit lines: $y_L(x)$

Since line spacing varies within the periphery, the length of transit lines at x is: $4\frac{2x}{s_r(x)^2}s_r(x) = \frac{8x}{s_r(x)}$. This holds where $x > r$ for y_L and all y below.

B.2. Global cost for length of the transit lines: F_L

Since line spacing is s_g in the central district, the global cost for the total length of the transit lines in that district, F_L, is: $\frac{4r^2}{s_g^2}\frac{4s_g}{2} = \frac{8r^2}{s_g}$.

B.3. Local cost for vehicle-distance traveled per hour: $y_V(x)$

The average ratio of the total distance traveled to the perpendicular travel distance is $\frac{3}{2}$, as shown in Daganzo (2010). Thus, the vehicle-distance traveled per hour at x in the periphery (i.e. $y_V(x)$) is: $2 * 4\frac{2x}{s_r(x)H_r(x)}\frac{3}{2} = \frac{24x}{s_r(x)H_r(x)}$.

B.4. Global cost for vehicle-distance traveled per hour: F_V

Since headway in the central district is H_g, the vehicle-distance traveled per hour in that district is: $\frac{16r^2}{s_g H_g}$. The vehicle-distance traveled per hour on the outermost boundary ring is: $2\frac{8r}{H_B}$. The sum of the two components is the global cost for vehicle-distance traveled per hour, F_V: $\frac{16r^2}{s_g H_g} + \frac{16r}{H_B}$.

B.5. Local cost for fleet size in the rush: $y_M(x)$

As in Appendix B, fleet size is the ratio of the total distance traveled per hour to the commercial speed. Thus, $y_M(x)$ is: $\frac{24r}{s_r(x)H_r(x)v_{cr}(x)}$.

B.6. Global cost for fleet size in the rush: F_M

Much as in C.5, the global cost for fleet size in the rush, F_M, is: $\frac{16r^2}{s_g H_g v_{ci}} + \frac{16r}{H_B v_{cB}}$.

B.7. Global cost for expected number of transfers per trip: $Fe_T = 1 + \frac{1}{2}(\int_r^R P_o(y)dy \int_r^R P_d(y)dy)$

This expected value is estimated as in Daganzo (2010), except that we modify it to account for the possibility of non-uniformly distributed demand for travel.

B.8. Local cost for waiting time: $y_W(x) = (P_o(x) + P_d(x))\frac{H_r(x)}{2}$

The local cost for waiting time includes the time waiting at the origin stop at x (i.e. $P_o(x)\frac{H_r(x)}{2}$), and the time at the destination stop (i.e. $P_d(x)\frac{H_r(x)}{2}$).

B.9. Global cost for waiting time: $F_W = \int_0^{d/2}(P_o(x) + P_d(x))\frac{H_g}{2}dx + \frac{1}{4}(\int_r^R P_o(y)dy \int_r^R P_d(y)dy)(\frac{H_g}{2} + \frac{H_B}{2})$

The waiting time in the central area is: $\int_0^{d/2}(P_o(x) + P_d(x))\frac{H_g}{2}dx + \frac{1}{4}(\int_r^R P_o(y)dy \int_r^R P_d(y)dy)\frac{H_g}{2}$. The waiting time on the boundary route is $\frac{1}{4}(\int_r^R P_o(y)dy \int_r^R P_d(y)dy)\frac{H_B}{2}$. The sum is the global cost for waiting time.

B.10. Local cost for access time: $y_A(x) = (P_o(x) + P_d(x))(\frac{s_r(x)}{4w} + \frac{s}{4w})$

The expected access distance in the periphery is $\frac{s_r(x)}{4} + \frac{s}{4}$. This value, weighted by the travel demand, is the local cost for access time, $y_A(x)$.

B.11. Global cost for access time: $F_A = (P_o(x) + P_d(x))(\frac{ss_g}{s+s_g}\frac{1}{4w} + \frac{s_g}{4w})$

As in Appendix B, $\frac{ss_g}{s+s_g}$ is used as the average stop spacing in the central district. Thus, the expected access distance in that district is: $\frac{ss_g}{s+s_g}\frac{1}{4} + \frac{s_g}{4}$. The global cost for access time is obtained by weighting the latter value by the travel demand.

B.12. Local cost for expected in-vehicle travel time: $y_T(x)$

The local cost for in-vehicle travel time per trip, $y_T(x)$, is: $(P_o(x) + P_d(x))(x - r)\frac{3}{2}\frac{1}{v_{cr}(x)}$, where the factor $\frac{3}{2}$ is the same ratio used in C.3.

B.13. Global cost for expected in-vehicle travel time: $F_T = 2R(\frac{\alpha}{12})[(11-\alpha^2)(1-\alpha^4)+8\alpha^4]\frac{1}{v_{ci}}\frac{\int_0^r (P_o(x)+P_d(x))dx}{2\alpha^2} + (\int_r^R P_o(y)dy \int_r^R P_d(y)dy)\frac{1}{4}\frac{2r}{3v_{cB}}$

The expected in-vehicle travel time per trip inside the central district is obtained by multiplying the result in Daganzo (2010) for uniformly-distributed travel demand, $2R(\frac{\alpha}{12})[(11-\alpha^2)(1-\alpha^4)+8\alpha^4]\frac{1}{v_{ci}}$, by the factor $\frac{\int_0^r (P_o(x)+P_d(x))dx}{2\alpha^2}$ to account for the possibility of non-uniformly distributed travel demand. The expected in-vehicle travel time per trip on the boundary route is: $(\int_r^R P_o(y)dy \int_r^R P_d(y)dy)\frac{1}{4}\frac{2r}{3v_{cB}}$, where $\frac{2r}{3}$ is the average travel distance on that route. The sum is the global cost for expected in-vehicle travel time.

B.14. Commercial speed v_{ci}, v_{cB}, and $v_{cr}(x)$

The commercial speed in the central district, v_{ci}, is determined by (i) cruising time, $\frac{1}{v_g}$; (ii) the time lost at stations due to acceleration and deceleration, $\tau(\frac{1}{s_g}+\frac{1}{s})$; and (iii) the time spent boarding patrons, $\tau'\Lambda(\alpha^2+1+\frac{1}{4}(\int_r^R P_o(y)dy \int_r^R P_d(y)dy))\frac{s_g H_g}{16r^2}$. Hence, we find that $v_{ci} = 1/(\frac{1}{v_g}+\tau(\frac{1}{s_g}+\frac{1}{s})+\tau'\Lambda(\alpha^2+1+\frac{1}{4}(\int_r^R P_o(y)dy \int_r^R P_d(y)dy))\frac{s_g H_g}{16r^2})$.

Commercial speed on the boundary route, v_{cB}, is also dependent on the above three factors. Hence, $v_{cB} = 1/(\frac{1}{v_B}+\tau(\frac{1}{s}+\frac{1}{s_r(r)})+\tau'\Lambda[\int_r^R P_o(y)dy \int_r^R P_d(y)dy]\frac{H_B}{64r})$

Commercial speed in the periphery, $v_{cr}(x)$, is also dependent upon the above three factors and varies with x. Hence, $v_{cr}(x) = 1/(\frac{1}{v_r(x)}+\tau\frac{1}{s}+\tau'\Lambda\frac{8x}{4R^2}\frac{H_g s_g}{24r})$.

B.15. Vehicle's passenger-carrying capacity constraint on boundary route

As in the Appendix B, the total number onboard all vehicles on the boundary line is: $\Lambda(\int_r^R P_o(y)dy \int_r^R P_d(y)dy)\frac{1}{4}$. The flow of transit vehicles on that boundary is: $\frac{2}{H_B}$. And the ratio of the average trip length to the length of the boundary line is: $\frac{1}{12}$. Hence, the expected maximum number of passengers in a vehicle on the boundary line, O_B, is: $\Lambda(\int_r^R P_o(y)dy \int_r^R P_d(y)dy)\frac{1}{4}\frac{2}{H_B}\frac{1}{12}$. And the vehicle's passenger-carrying capacity constraint on the boundary is: $O_B - C_{pax} < 0$.

The passenger-carrying capacity constraints for the central district and the periphery are as in Daganzo (2010).

B.16. Vehicle conservation constraint

In the periphery, the vehicle conservation constraint is the same as in the ring-radial network, see appendix A.1.

In the central district, the total vehicle flow is $\frac{8r}{s_g H_g}$. Because all the buses travel to/from the city's boundary, the vehicle conservation constraint in the central district is $Q = \frac{8r}{s_g H_g}$.

References

Badia, Hugo., Estrada, Miquel., and Robuste, Francesc., 2014. Competitive Transit Network Design in Cities with Radial Street Patterns. *Transportation Research Part B* (59),2014 pp 161–181.

Black, A., 1979. Optimizing Urban Mass Transit System: A General Model. *Transportation Research Record*, 677, 41–47.

Byrne, B.F., 1975. Public Transportation Line Positions and Headways for Minimum User and System Cost in A Radial Case. *Transportation Reseaerch*. Vol. 9, pp. 97–102.

Chen, H., Gu, W., Cassidy, M., and Daganzo, C.F., 2014. Continuum Approximation Method of Designing Transit to Serve Ring-radial and Grid Streets. *Tech Report*.

Clarens, G., and Hurdle, V.F., 1975. An Operating Strategy for A Commuter Bus System. *Transportation Science*. 9 (1), 1–20.

Daganzo, C.F., 2010. Structure of Competitive Transit Networks. *Transportation Research Part B*(44), 2010 pp 434–446

Daganzo, C.F., 2010a. Public Transportation Systems: Basic Principles of System Design, Operations Planning and Real-Time Control. *Course Notes UCB-ITS-CN-2010-1*.

Estrada, M., Roca-Riu, M., Badia, H., Robust, F., and Daganzo, C.F., 2011. Design and Implementation of Efficient Transit Networks: Procedure, Case Study and Validity Test, *Transportation Research Part A* 45 , 2011, 935950.

Fairthorne, D., 1963. The Distances Between Pairs of Points in Towns of Simple Geometrical Shapes. *Proceedings of the Second International Symposium on the Theory of Road Traffic Flow*, 391406.

Holroyd, E.M., 1966. Theoretical Average Journeys Lengths in Circular Towns with Various Routening Systems. *Volume 43 of RRL report: Road Research Laboratory*, 1966.

Holroyd, E.M., 1967. The Optimum Bus Service: A Theoretical Model for A Large Uniform Urban Area. Proceedings of the Third International Symposium on the Theory of Traffic Flow, 1967, p. 308-328

Newell, G.F., 1971. Dispatching Policies for A Transportation Route. Transportation Science. 5, 91-105.

Newell, G. F., 1973. Scheduling, Location, Transportation, and Continuum Mechanics; Some Simple Approximations to Optimization Problems. *SIAM J. Appl. Math*. 25 (3), 346-360.

Newell, G.F., 1979. Some Issues Relating to the Optimal Design of Bus Routes. *Transportation Science* 13(1), 2035.

Ouyang, Y., Daganzo, C.F., 2006. Discretization and validation of the continuum approximation scheme for terminal system design. *Transportation Science* 40, 89 - 98.

Vaughan, R., 1986. Optimum Polar Networks for An Urban Bus System with A Many-to-many Travel Demand. *Transportation Research, Part B: Methodology*, 20B(3), 215-224.

Wirasinghe, S.C. and Ghoneim, N.A., 1981. Spacing of Bus-stops for Many to Many Travel Demand. *Transportation Science*. 15, 210-221.